Antarctic Science 20 (6), 565–579 (2008) © Antarctic Science Ltd 2008 Printed in the UK doi:10.1017/S0954102008001375

The role of thermal contraction crack polygons in cold-desert fluvial systems

JOSEPH S. LEVY[1]*, JAMES W. HEAD[1] and DAVID R. MARCHANT[2]

[1]*Brown University Department of Geological Sciences, 324 Brook Street, Geological Sciences Box 1846, Providence, RI 02912, USA*
[2]*Department of Earth Sciences, Boston University, 675 Commonwealth Ave, Boston, MA 02215, USA*
**joseph_levy@brown.edu*

Abstract: Thermal contraction crack polygons modify the generation, transport, and storage of water in Wright Valley gullies. Water generation is contributed to by trapping of windblown snow in polygon troughs. Water transport is modified by changes to the ice-cement table and active layer topography caused by polygon trough formation. Water storage is modified by sediment grain-size distribution within polygons in gully distal hyporheic zones. Patterned ground morphological variation can serve as an indicator of fluvial modification, ranging from nearly unmodified composite-wedge polygons to polygons forming in association with gully channels. Thermal contraction crack polygons may also constrain the gully formation sequence, suggesting the continuous presence of permafrost beneath the Wright Valley gullies during the entire period of gully emplacement. This analysis provides a framework for understanding the relationships between polygons and gullies observed on Mars. If comparable stratigraphic relationships can be documented, the presence of an analogous impermeable ice-cemented layer beneath the gullies can be inferred, suggesting an atmospheric source for Martian gully-carving fluids.

Received 22 October 2007, accepted 4 February 2008

Key words: hyporheic zone, McMurdo Dry Valleys, microclimates, patterned ground, permafrost

Introduction

Although interactions between ice-wedge polygons and fluvial-lacustrine systems in the Arctic have received extensive treatment (Lachenbruch 1962, 1963), the effects of polygonal patterning on the generation and modification of cold-desert fluvial systems have not been broadly discussed, despite the observation of gullies in polygonally patterned terrains on Earth and Mars (Péwé 1974, McKnight *et al.* 1999, Bridges & Lackner 2006, Fortier *et al.* 2007). Thermal contraction crack polygons (hereafter, abbreviated as "polygons") are a set of geomorphological features that alter the distribution of ice and soil, and create a network of linear pathways for fluids and/or vapour (Marchant *et al.* 2002, Marchant & Head 2007). In areas where polygons occur in association with gullies, the redistribution of surface water in polygon troughs has important implications for the evolution of such gullies. In addition, the preferred flow of water in polygon troughs may alter the solute chemistry and biological potential of near-surface waters (e.g. Gooseff *et al.* 2002, Wentworth *et al.* 2003, Burt & Knauth 2007, Harris *et al.* 2007). Here, we present field measurements of a variety of composite-wedge polygons (defined below) in the South Fork region of Wright Valley that bear on the evolution and modification of gullies formed in cold-desert climates.

Geological setting

Upper Wright Valley

The South Fork of upper Wright Valley is centred at ~77°33'36"S, ~161°17'24"E, in the McMurdo Dry Valleys of southern Victoria Land (Fig. 1). Wright Valley extends from the margin of the East Antarctic Ice Sheet to the Ross Sea. Valley floor elevations span ~85 to 300 m and walls rise up to 1000 m above the valley floor. The bedrock is a Precambrian to Palaeozoic metamorphic complex, including granite gneisses, lamprophyre, rhyolite porphyry dikes, and Jurassic dolerite sills (Isaac *et al.* 1996).

Climatically, the floor of Wright Valley falls within the coastal thaw zone, as defined by Marchant & Head (2007), with portions of the upper walls transitioning into the inland mixed zone. Wright Valley is a cold desert, with a mean annual temperature of -20°C (Riordan 1973, Thompson 1973). Diurnal air temperatures recorded during the study interval (1 December–31 December 2006) fluctuated by as much as ~12°C, reaching a maximum of 9.4°C, and a minimum of -9.5°C; the daily mean temperature was -0.2°C. Relative humidity averaged 35%, confirming generally desiccating conditions (Ragotzkie & Likens 1964).

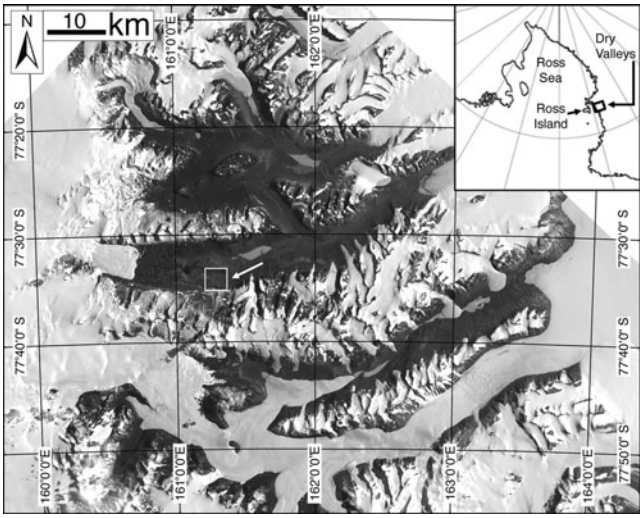

Fig. 1. Location map of Antarctic Dry Valleys in southern Victoria Land, Antarctica. The South Fork study site in upper Wright Valley is surrounded by a box and indicated with an arrow. Inset map shows the location of the McMurdo Dry Valleys on a map of the Ross Sea sector; south is towards inset top.

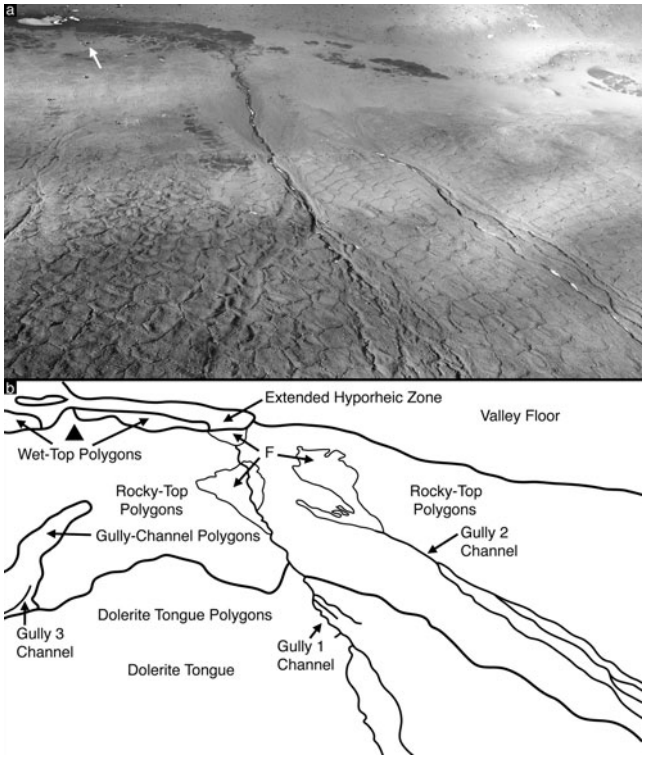

Fig. 2. a. Oblique, aerial view of the South Fork study site from the south, looking down-slope, to the north. Notable geomorphic surface features include gullies and thermal contraction crack polygons. A small, seasonal pond, ~30 m in the long axis, is visible in the upper left, above two Scott tents and an 8′ × 16′ Endurance tent (arrow). **b.** Sketch delimiting geomorphic units shown above. F indicates fan surfaces, Valley Floor indicates an unpatterned portion of the valley floor, and Dolerite Tongue indicates a tongue-shaped assemblage of dolerite boulders. The location of the campsite is marked with a triangle.

South Fork

The South Fork study area is bounded to the north by the Dais plateau, and to the west by a large slump block ~2 km long by ~600 m wide (Fig. 2). The valley floor is dominated by unconsolidated colluvium and glacial drifts; the latter are associated with advance of the Wright Upper Glacier. A seasonally moist active layer, 20–45 cm thick, overlies perennially frozen sands and gravels (pore ice < 30% by volume) (McGinnis & Jensen 1971, Head *et al.* 2007a), and thermal contraction crack polygons are widespread. Gullies, composed of a broad alcove, a narrow channel, and a distal fan, are common on the south valley wall (Dickson *et al.* 2007, Head *et al.* 2007a, Levy *et al.* 2007b, Morgan *et al.* 2007). Three mapped gullies occur in association with a broad, tongue-shaped lobe, capped by dolerite boulders, that extends from the valley rim down to the valley floor (here termed, "the dolerite tongue") (Fig. 2).

Morphological varieties of composite-wedge polygons

Thermal contraction crack polygons are ubiquitous in the McMurdo Dry Valleys (Berg & Black 1966, Marchant *et al.* 2002). All polygons arise initially from the failure of frozen ground in response to thermal tension induced by seasonal temperature change (Leffingwell 1915, Péwé 1959, Black 1982, Mellon 1997, McKay *et al.* 1998, Marchant *et al.* 2002, Marchant & Head 2007). Morphological changes thereafter are largely related to local microclimatic conditions: principally soil moisture distribution, and whether or not ice, sand, or a combination of the two fill marginal polygon troughs and underlying cracks. In the case of composite-wedge polygons, the principal polygon examined here, thermal-contraction cracks are filled with alternating lenses of ice and sand; this contrasts sharply with typical ice-wedge polygons that contain marginal wedges of concentrated ice (Berg & Black 1966). At the surface, clusters of composite-wedge polygons form fractures that intersect at diagnostic angles (typically near-120°, "hexagonal" intersections, or near-90°, "orthogonal" intersections) (Lachenbruch 1962).

A schematic illustration of typical composite-wedge polygon morphology is provided in Fig. 3. The polygon interior is defined as the polygon-shaped surface bounded by thermal contraction cracks. The polygon trough is defined as the surface expression of the composite-wedge; troughs are commonly lower in elevation than polygon interiors. Raised shoulders are defined as elevated portions of the polygon interior immediately adjacent to the polygon trough; these may arise from compressive stresses associated with infill of the polygon wedge. The wedge is the subsurface expression of multiple episodes of thermal

https://doi.org/10.1017/S0954102008001375 Published online by Cambridge University Press

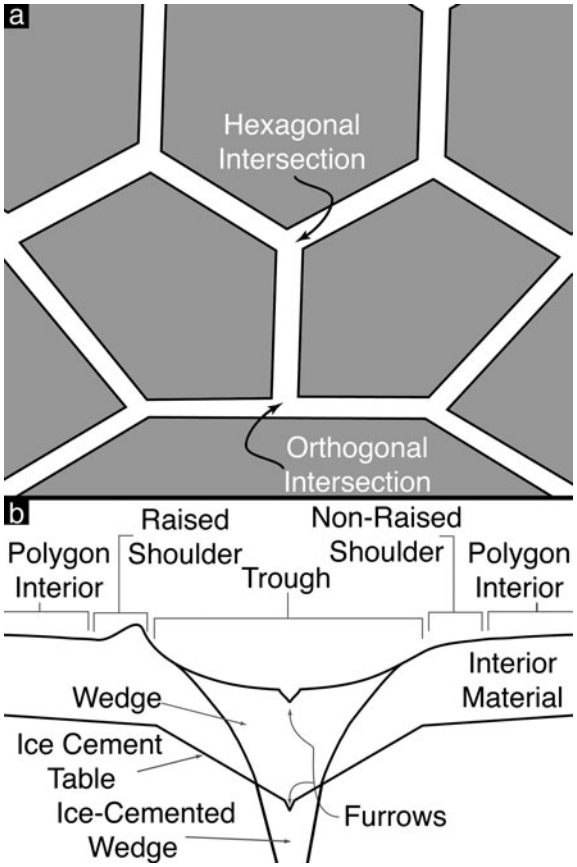

Fig. 3. a. Schematic plan-view of thermal contraction crack polygons. Polygon interiors are shaded; polygon troughs are unshaded. Typical "hexagonal" (near-120°) and "orthogonal" (near-90°) trough intersections are illustrated. **b.** Schematic cross-section of the subsurface structure of a typical composite-wedge polygon.

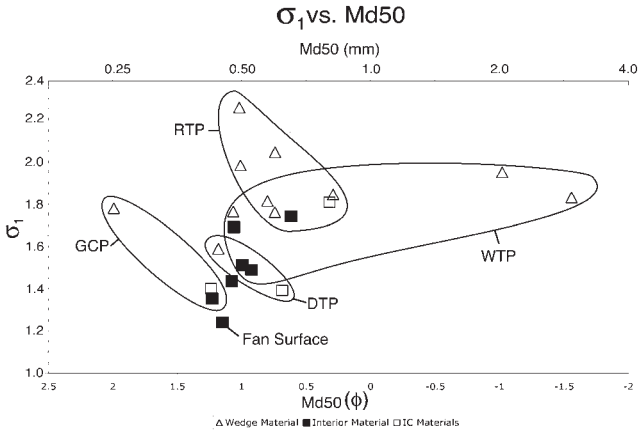

Fig. 4. Plot of grain-size inclusive standard deviation (σ_1) versus median grain size, determined by mass (Md50). σ_1 is an indication of the degree of soil sorting, with higher values indicating poorer sorting (Masch & Denny 1966). RTP indicates rocky-top polygons, DTP indicates dolerite-tongue polygons, GCP indicates gully-channel polygons, WTP indicates wet-top polygons, fan surface indicates material sampled from the gully 2 fan surface, and IC materials indicates ice-cemented sediments.

contraction crack expansion, and the subsequent winnowing down of overlying sediments and/or meltwater, producing vertically laminated sediments mixed with ice. Furrows are defined as shallow, linear depressions, either at the trough surface or at the buried-ice-cement surface, indicative of local winnowing (in the trough) or expansion of the thermal contraction crack (in the ice-cement) by sublimation. The ice-cement is the competent substrate in which thermal contraction cracking occurs, producing the polygons. Ice-cement table depth generally follows surface topography. Interior material is defined as the unconsolidated regolith present at the polygon centre.

Several variations on this idealized composite-wedge polygon morphology are present in South Fork. As shown below, variation reflects changes in substrate composition, surface slope, surface cover, water content, and soil catena, driven by increasing degrees of fluvial modification from gully interactions. For each morphological variety of composite-wedge polygon examined, we present a description of its surface manifestation and its subsurface structure; the former derived from ground and air observations, the latter from soil pit excavation, gravimetric water content ("GWC") analysis and dry sieving of samples. Gravimetric water content (GWC) is calculated as

Table I. Summary of physical characteristics of composite-wedge polygon morphological varieties present in the South Fork study area.

Polygon morphological variety	Diameter[1]	Trough width[1]	Intersection type	Centre surface	Trough surface
Dolerite-tongue polygons (DTP)	12–24 m (16 m)	0.8–1.3 m (mean 1.1 m)	Near-90°	Dolerite boulders and cobbles over coarse sand	Dolerite boulders and cobbles, gravitationally sorted
Rocky-top polygons (RTP)	6.5–16.5 m (11.0 m)	0.2–1.6 m (mean 0.7 m)	Mostly near-120°, some near-90°	Dolerite and granite cobbles over coarse sand	Coarse sand and small pebbles
Gully-channel polygons (GCP)	Variable, on scale of RTP and DTP	1–2 m, channel-dependent	Near-90°	Dolerite cobbles and boulders over medium sand, commonly bedded	Small dolerite cobbles and pebbles over medium sand
Wet-top polygons (WTP)	10–20 m (16 m)	0.2–2.0 m (mean 1.0 m)	Near-120°	Dolerite cobbles and boulders over wet, coarse sand	Granite pebbles

[1]Mean value in parentheses, $n = 20$.

https://doi.org/10.1017/S0954102008001375 Published online by Cambridge University Press

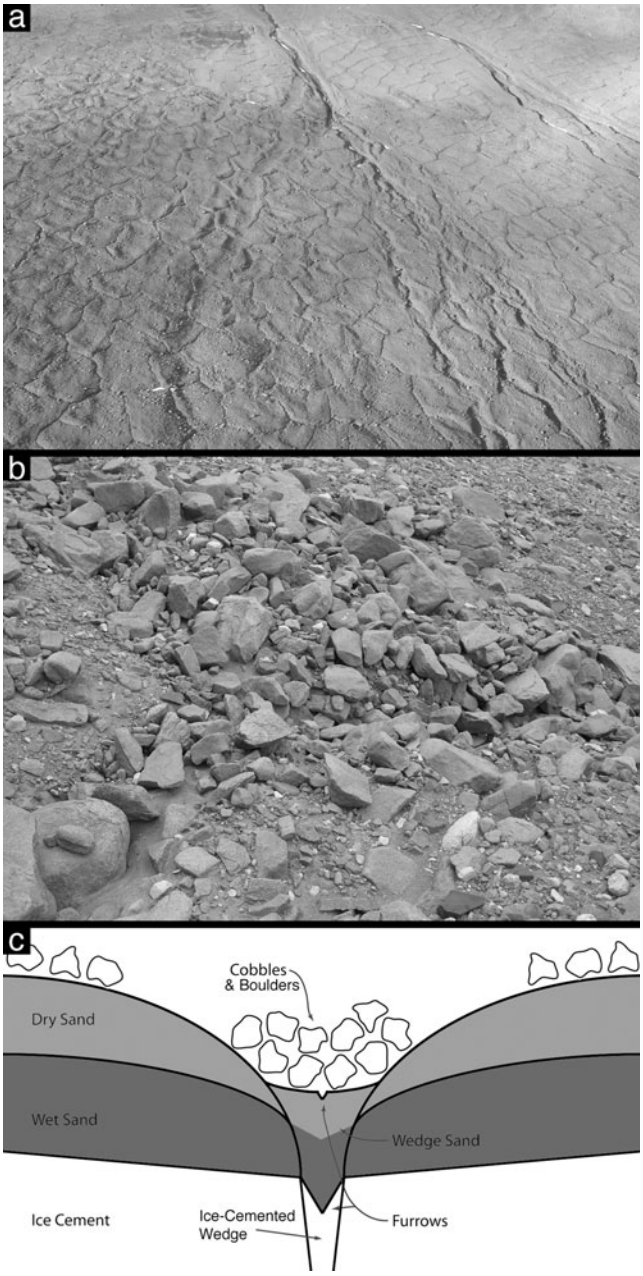

Fig. 5. a. Dolerite-tongue polygons viewed from the air. Mean dolerite-tongue polygon diameter is 16 m. **b.** Dolerite-tongue polygons viewed from the surface. Dolerite-tongue polygon troughs have a mean width of 1.1 m. **c.** Schematic cross section of a dolerite-tongue polygon.

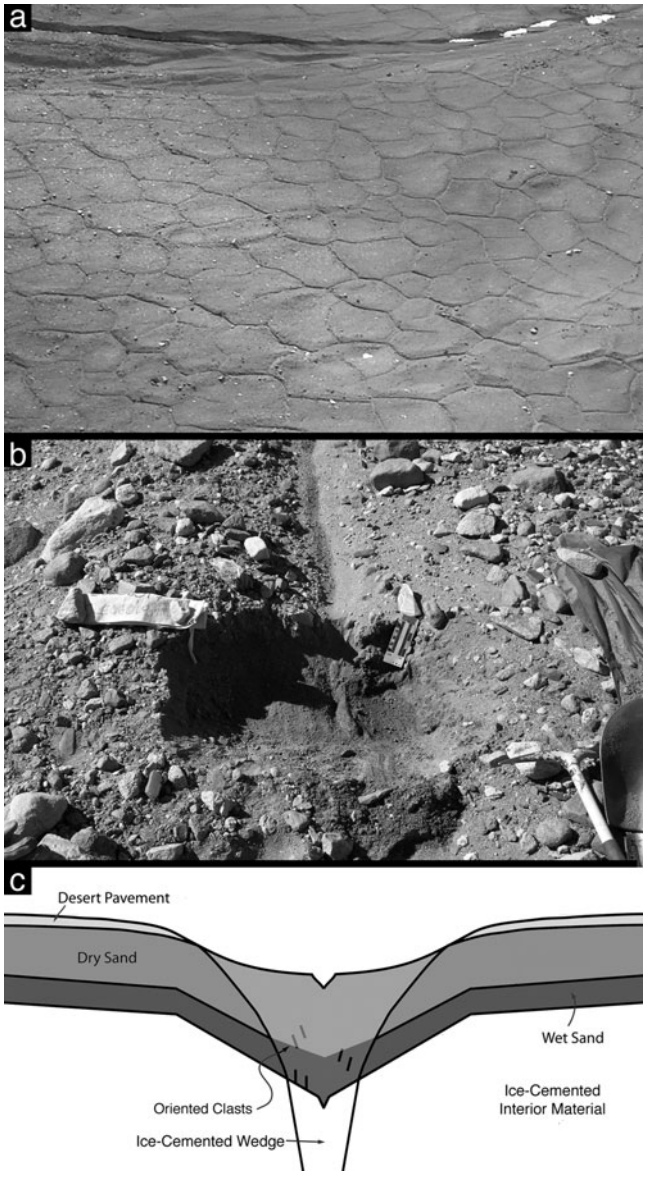

Fig. 6. a. Aerial view of rocky-top polygons. Mean rocky-top polygon diameter is 11 m. **b.** Excavation of a rocky-top polygon. The rocky-top polygon trough is oriented vertically. Rocky-top polygon troughs have a mean width of 0.7 m. An ice-cemented composite-wedge is visible at centre. **c.** Schematic cross section of a rocky-top polygon.

the percent ratio of the mass of water in a sample to the mass of the dry sample after baking at 105°C for 12 hours (Topp 1993). Grain size analyses are presented in terms of d_x, where d is a grain diameter in ϕ units ($\phi = -\log_2$[diameter in mm]) and x is the percentage of the sample finer than the given diameter, d (e.g. Sheldrick & Wang 1993). A summary of these results is found in Table I and Fig. 4.

Dolerite-tongue polygons

Composite-wedge polygons within the prominent dolerite tongue at the southern edge of the study site are here termed dolerite-tongue polygons (Figs 2 & 5). Surficially, dolerite-tongue polygons are composed primarily of near-90° trough intersections, oriented down- and cross-slope, forming polygons 12–24 m in diameter (mean diameter = 16 m). Dolerite-tongue polygon trough widths span 0.8–1.3 m (mean width = 1.1 m) at the surface, and are commonly depressed ~30 cm or deeper (up to ~1 m) relative to

https://doi.org/10.1017/S0954102008001375 Published online by Cambridge University Press

polygon interiors. Dolerite-tongue polygons do not show raised rims. Dolerite-tongue polygon troughs are partially filled by coarse sand and pebbles, and capped by dolerite boulders, commonly at least 50 cm in diameter. Few boulders are present along trough shoulders, suggesting gravitational sorting of larger blocks into the troughs. Shallow, 1–2 cm wide surficial axial furrows are common at the bottom of dolerite-tongue polygon troughs, which, along with the presence of sand funnels, suggests current expansion of some dolerite-tongue polygon thermal contraction cracks and winnowing of underlying sediments.

Dolerite-tongue polygons have a structure similar to that of typical composite-wedge polygons. Measured depths to the ice-cement table range between 20–23 cm in dolerite-tongue polygons. Axial furrows at least 1–2 cm deep cut into the ice-cemented portions of dolerite-tongue polygon wedges, suggesting recent fracture expansion. Overlying the ice-cemented sediment in both the polygon wedge and interior (GWC = 13.2%) is a layer of dark, seasonally moist sand (GWC = 11.0%) 10–15 cm thick, which is overlain by ~10 cm of dry sand (GWC = 0.7%). At dolerite-tongue polygon interiors, this dry sand (d_{50} = 0.99, d_{84} = -0.78) is overlain by dolerite boulders and cobbles ~0.2–2 m in diameter.

Rocky-top polygons

Composite-wedge polygons present on the valley floor and lower valley walls in South Fork constitute the rocky-top polygon variety (Figs 2 & 6). Surficially, rocky-top polygons are composed primarily of near-hexagonal trough intersections, although some near-orthogonal intersections are present, forming polygons 6.5–16.5 m in diameter (mean diameter = 11.0 m). Rocky-top polygon troughs span 0.2–1.6 m in width (mean width = 0.7 m) at the surface, and are commonly depressed 5–15 cm below polygon interiors (being generally deeper at trough intersections and shallower mid-trough). Rows of ~10 cm cobbles line some rocky-top polygon troughs, and slightly raised shoulders (> 5 cm relief relative to rocky-top polygon interiors) are present along some troughs. Some rocky-top polygon troughs are substantially curved in plan view, having displacements of 0.5–1 m over 5 m lengths of trough. Shallow, 1–2 cm wide axial surface furrows are common in rocky-top polygon troughs, which, along with the presence of sand funnels, suggests winnowing of sediments.

Rocky-top polygons have a relatively simple structure, similar to typical composite-wedge polygons. Measured depth to the ice-cement table ranges between 20–30 cm in rocky-top polygons; however, ice-cemented wedge materials can rise to within 1 cm of the surface when troughs are filled with wind blown snow. Overlying ice-cemented rocky-top polygon interior material (GWC = 3.4–4.7%) is a layer of dark, seasonally moist sand (GWC = 1.8%), which, in turn, is overlain by 10–20 cm of dry sand (GWC = 1.3%). Rocky-top polygon interiors are covered by fine grained dolerite cobbles (3–8 cm in diameter) and granite cobbles (commonly 10–20 cm in diameter), forming a desert

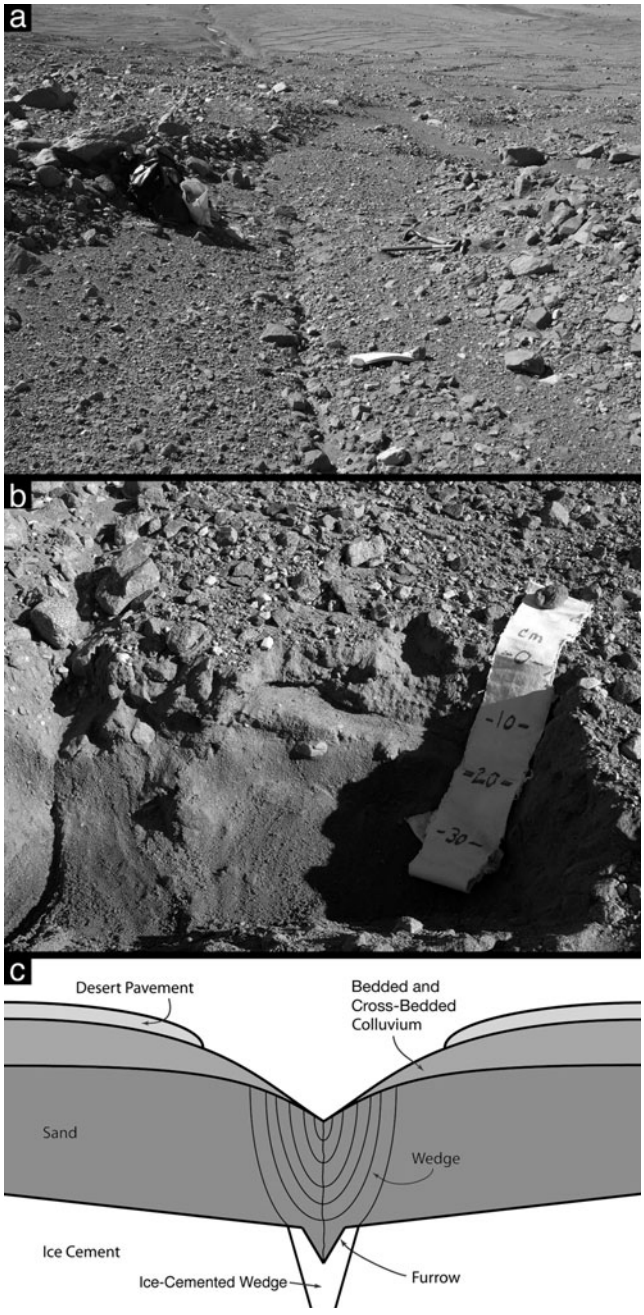

Fig. 7. a. Surface view of a gully-channel polygon, looking downslope. **b.** Excavation into a gully-channel polygon showing desert pavement overlying slightly indurated, bedded and cross-bedded sediments interpreted to be a fluvial deposit. A broad wedge of vertically laminated sand is visible below the fluvial sediment, associated with an actively expanding fracture visible at left. **c.** Schematic cross-section of a gully-channel polygon.

https://doi.org/10.1017/S0954102008001375 Published online by Cambridge University Press

pavement over the dry sand ($d_{50} = 1.08$, $d_{84} = -0.54$). In rocky-top polygon wedges, axial furrows 1–2 cm deep are common in the ice-cemented portion of the wedge. Overlying the ice-cemented portion of the wedge is coarse sand to fine gravel ($d_{50} = 0.80$, $d_{84} = -1.70$), which is moist (GWC = 2.5%) for the lower ~10 cm, and dries towards the surface (GWC = 1.1%). Cobbles present in the ice-cemented, as well as in the unconsolidated portions of the wedge, are commonly oriented vertically, suggesting in-fall or winnowing associated with crack expansion.

Gully-channel polygons

Composite-wedge polygons present in the upper reaches of the channels of gullies 1–3 constitute the gully-channel polygon morphological variety (Figs 2 & 7). Surficially, gully-channel polygons are composed primarily of near-orthogonal trough intersections, forming polygons of comparable diameter to rocky-top polygons and dolerite-tongue polygons. Gully-channel polygons are principally identified by the presence of broadened troughs (1–2 m in width), localized in inactive gully channels, composed of reworked colluvial material, commonly depressed 10–15 cm below polygon interiors. Furrows, 5–10 cm wide and 3–5 cm deep, are common in gully-channel polygon troughs, trending both axially and transversely to the trough. Surface furrows suggest the recent expansion of some gully-channel polygon cracks and winnowing of overlying sediments.

Gully-channel polygon subsurface structure is significantly different from typical composite-wedge polygon structure. Measured depth to the ice-cement table ranges between 20–30 cm in gully-channel polygons. The ice-cemented portion of the wedge commonly contains an axial furrow, 1 cm deep and 1 cm wide. Overlying ice-cemented sediment (GWC = 10.4%) is a layer of dark, seasonally moist sand (GWC = 3.6%) 18–20 cm thick ($d_{50} = -1.16$, $d_{84} = 0.11$). This moist sand is overlain by 10–15 cm of dry, bedded, cross-bedded, and slightly indurated sediment (GWC = 0.9%) ($d_{50} = 1.23$, $d_{84} = -0.15$). Dry medium to coarse sand (GWC = 0.5%) occupies the upper 5 cm of gully-channel polygons ($d_{50} = -1.26$, $d_{84} = 1.43$). Dolerite cobbles and pebbles form a desert pavement over gully-channel polygons, with clasts ranging in size from, 3–10 cm in diameter over troughs, 10–100 cm in diameter over the polygon interiors.

The presence of horizontally bedded and cross-bedded sediment in broad troughs, suggests that gully-channel polygons are relict gully channels which no longer transport water along the surface. The presence of vertically laminated wedges beneath horizontally stratified fluvial sediments suggests that the polygon troughs predate the deposition of bedded sediment. The presence of surface furrows dissecting overlying colluvium and desert pavement suggests that some gully-channel polygon fractures are currently expanding.

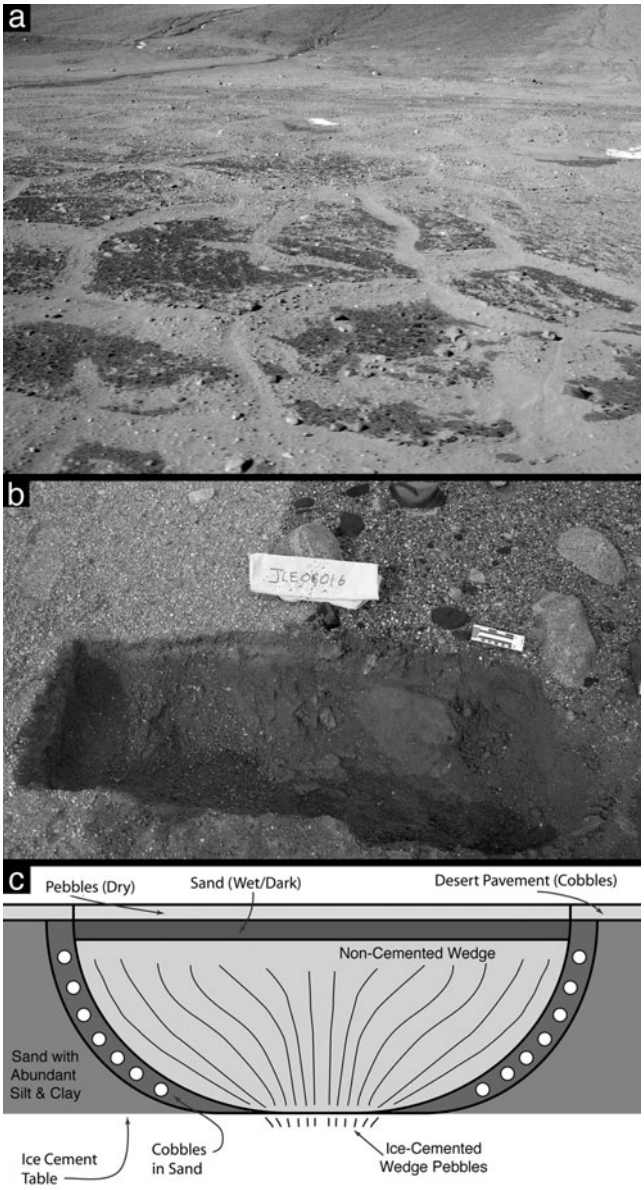

Fig. 8. a. Ground view of wet-top polygons in the distal hyporheic zone of gully 1. Wet-top polygons have a mean diameter of 16 m. Open furrows are visible, but are uncommon. **b.** Excavation into the contact between a wet-top polygon interior and wedge. **c.** Schematic cross-section of wet-top polygon subsurface structure.

Wet-top polygons

Composite-wedge polygons present in the distal hyporheic zone of gully 1 (McKnight *et al.* 1999, Levy *et al.* 2007a) constitute the wet-top polygon morphological variety (Figs 2 & 8). Wet-top polygons are delineated primarily by

https://doi.org/10.1017/S0954102008001375 Published online by Cambridge University Press

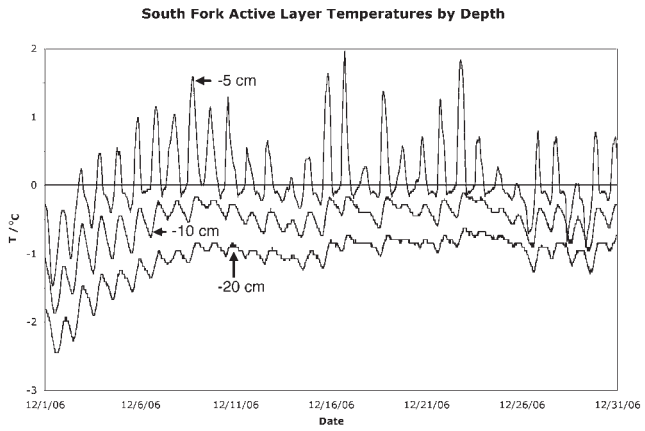

Fig. 9. Plot of ground temperature at several depths versus time in a rocky-top polygon interior adjacent to the gully 1 channel (77°33'52"S, 161°17'23"E) for the month of December 2006. Even at peak summer warming, the 0°C isotherm never penetrated deeper than 10 cm below the surface.

near-hexagonal trough intersections, forming polygons 10–20 m in diameter (mean diameter = 16 m). Wet-top polygon trough widths span 0.2–2.0 m (mean width = 1.0 m) at the surface, and have little to no topographic relief relative to polygon interiors. Axial furrows at the trough surface are rare. A striking albedo difference marks the surface contact between wet-top polygon troughs and interiors, caused primarily by differences in moisture content. The uppermost surfaces of wet-top polygon interiors are dark (GWC = 4.6–4.9%) and wet-top polygon trough surfaces are bright (GWC = 0.3–0.4%). Some wet-top polygon interior-trough contacts are marked by a single row of ~10 cm dolerite cobbles. Wet-top polygon interiors are covered by dolerite and granite pebbles and cobbles ~1–25 cm in diameter, overlying coarse sand to very fine gravel (d_{50} = 1.07, d_{84} = -1.85).

Wet-top polygons have a complex subsurface structure, resulting in part from their presence in the active hyporheic zones of the gullies. Depth to the ice-cement table ranges between 20–25 cm in wet-top polygons. The ice-cemented sediment in the interior of wet-top polygons is a brownish-red sand (d_{50} = 0.92, d_{84} = -0.66), with up to 2.2% fines (silts and clays) - the highest percentage of fines measured in any sample analysed (GWC = 8.9%). Moist, brownish-red sediment is present in wet-top polygon interiors above the ice-cement table (GWC = 3.6–3.9%). Between wet-top polygon interiors and wedges is a sloping assemblage of sand and ~10 cm cobbles. Axial furrows are rare in the ice-cemented portion of wet-top polygon wedges, which are composed predominantly of vertically bedded pebbles (GWC = 1.4%). Uncemented wedge material is composed primarily of light coloured pebbles, and in aggregate has GWC = 1.3–1.8%. Above wet-top polygon wedges is a 1–2 cm thick layer of dark sediment composed of coarse sand and pebbles (d_{50} = 1.07, d_{84} = -1.85) (GWC = 1.0%). Wet-top polygon troughs are surfaced by light-coloured, fine to very fine granite gravel (d_{50} = -1.02, d_{84} = 2.79) (GWC = 0.3–0.4%).

Fig. 10. Wind blown snowbank accumulated in a rocky-top polygon trough. Pick is 60 cm long.

Polygon-gully interactions

The presence of polygonally patterned ground over all components of the South Fork gully systems - the alcoves, channels, and fans (Malin & Edgett 2001, Head *et al.* 2007a) - opens up the possibility that polygons play a role in the accumulation, transport, and storage of water in gully systems. We draw on morphological evidence to link the polygons described above to one or more of these gully-forming processes.

Snow accumulation

Previous work has shown that the primary sources of water flowing through South Fork area gullies are summer melting of perennial snowpack in gully alcoves and melting of wind blown snow in gully channels (Dickson *et al.* 2007, Levy *et al.* 2007a, Morgan *et al.* 2007). The melting of ice-cemented sediment is not thought to significantly contribute to gully and active layer flow, as the 0°C isotherm did not penetrate deeply enough into the subsurface to encounter the ice-cement table during December 2006 (Fig. 9). Gully 1 is approximately 900 m long and sustains snowbanks of ~0.3 m thickness in a

https://doi.org/10.1017/S0954102008001375 Published online by Cambridge University Press

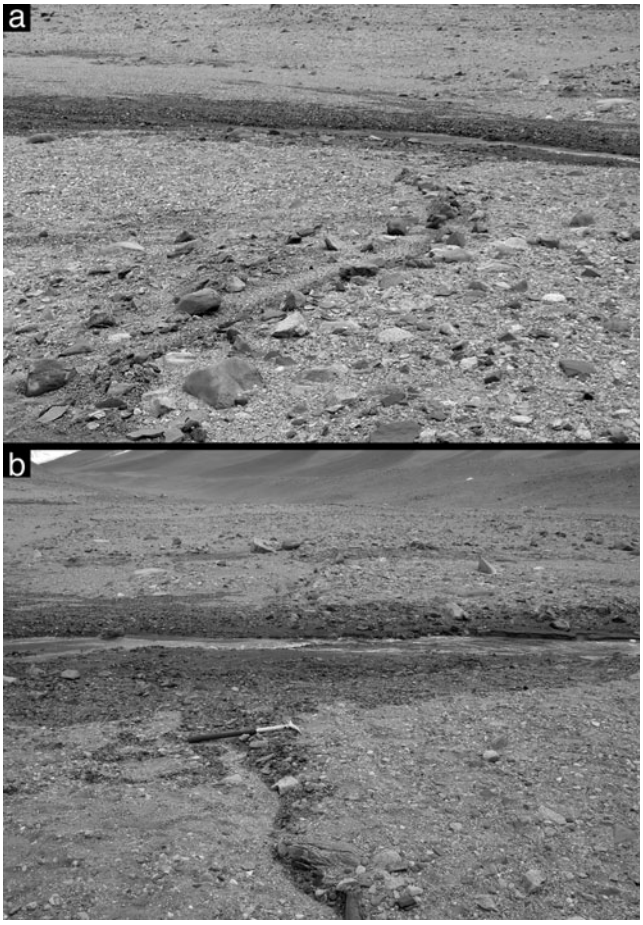

Fig. 11. a. and **b.** Darkened, moist trough material at the surface of rocky-top polygon troughs intersecting the gully 1 channel.

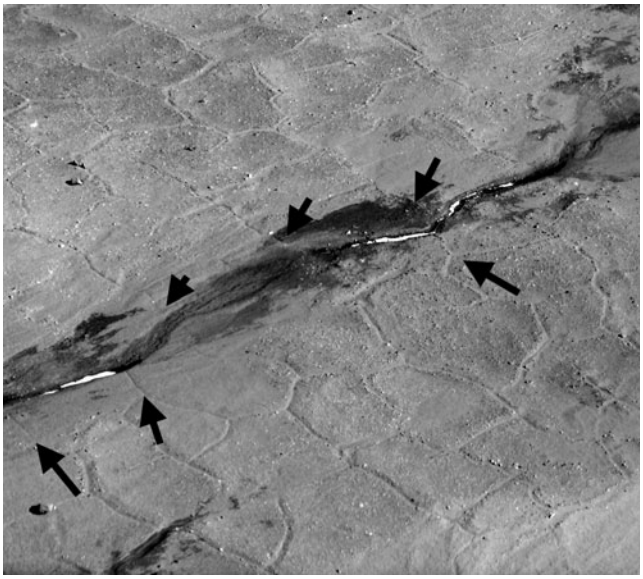

Fig. 12. Aerial view of a portion of the gully 1 channel. Arrows indicate rocky-top polygon troughs which directly intersect the gully channel.

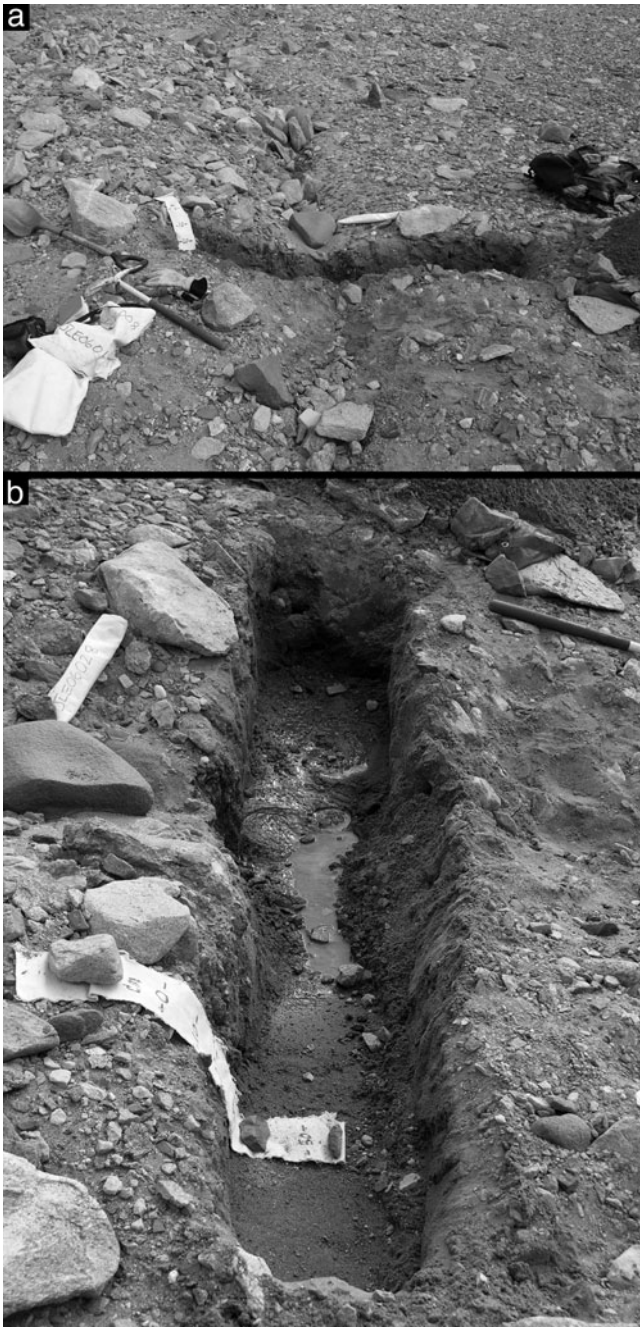

Fig. 13. a. Excavation into a rocky-top polygon trough on the southern valley wall of the study site. Upslope is to the south, towards image top. Pick to image left is 60 cm in length. **b.** View into the rocky-top polygon excavation shown in part a), looking west (vantage point is near shovel blade in part a). Water is flowing out of wedge material along the ice-cement table beneath the rocky-top polygon trough centre, and is being channelized by the local low created by the depressed ice-cement table. No flow is occurring along the ice-cement table beneath the rocky-top polygon interior.

https://doi.org/10.1017/S0954102008001375 Published online by Cambridge University Press

channel ~1 m wide (Fig. 2). Assuming complete filling of the channel (modelled as an inverted triangular prism), ~135 m^3 of snow is available for melting and flow.

Wind blown snow also accumulates in the troughs of thermal contraction crack polygons (Fig. 10). If this snow melts over the course of the summer, it too may be transported to gully channels (see following section), and augment gully flow (Figs 10–12). We estimated the amount of snow contributed to Gully 1 by polygons by calculating the maximum amount of snow that could be contained in rocky-top polygon and dolerite-tongue polygon troughs intersecting the gully 1 channel. We modelled the maximum dimensions of each wind blown snowbank as an inverted triangular prism, with dimensions equal to mean polygon trough length, width, and depth (Table I). The width and height are minimum values, as snowbanks were observed to overflow rocky-top polygon troughs. This simplified calculation estimates maximum accumulations of ~6 m^3 of snow within the 30 rocky-top polygon troughs that intersect the lower channel of gully 1, and ~240 m^3 of snow within the 45 dolerite-tongue polygons intersecting the upper reaches of the gully 1 channel. Thus, depending on the seasonal snow delivery to the South Fork study area, and the distribution of that snow among the polygon varieties present, volumes of snow approaching or exceeding the volume of wind blown snow accumulated in gully channels can be contributed to gully systems by the surrounding polygons.

Water transport

The presence of gully-channel polygons in the South Fork area strongly suggests that polygons have been involved in the transport process of water through gully systems. Previous work has shown that the ice-cement table provides an impermeable layer within 0.5 m of the surface, above which water can flow (Lyons *et al.* 2005, Head *et al.* 2007b, Levy *et al.* 2007a). What changes to the near-surface hydraulic regime are caused by patterned ground, and how do these changes affect gully activity and evolution?

Soil excavations in the South Fork study area revealed water flowing through the active layer along the surface of the ice-cement table (Fig. 13). Water percolated out of the base of the upslope walls of these excavations, from the ice-cement table to a height of ≤ 15 cm, slowly filling the excavation to the depth of the saturated layer, until equilibrium was established between inflow and outflow in the excavation. Flow was observed primarily in the active layer beneath polygon troughs on steep slopes, and across polygon troughs and interiors on shallow slopes. Water temperatures were measured and were found to be close to 0°C on 31 December 2006. Slow flow rates suggest that this water may be saline.

Subsurface topography of the ice-cement table also plays a role in dictating water flow. Water travelling through the active layer, along the ice-cement table beneath a polygon interior, will eventually encounter a polygon trough. Meltwater will drain down the locally steepened ice-cement table, toward the polygon trough, and thereafter will follow the ice-cement gradient in the trough down-slope. So long as the trough network remains generally oriented down-slope, water will remain channelled in ice-cemented polygon troughs. Where meltwater has access to gully channels, either by direct down-slope transport through single polygon troughs, through a network of linked

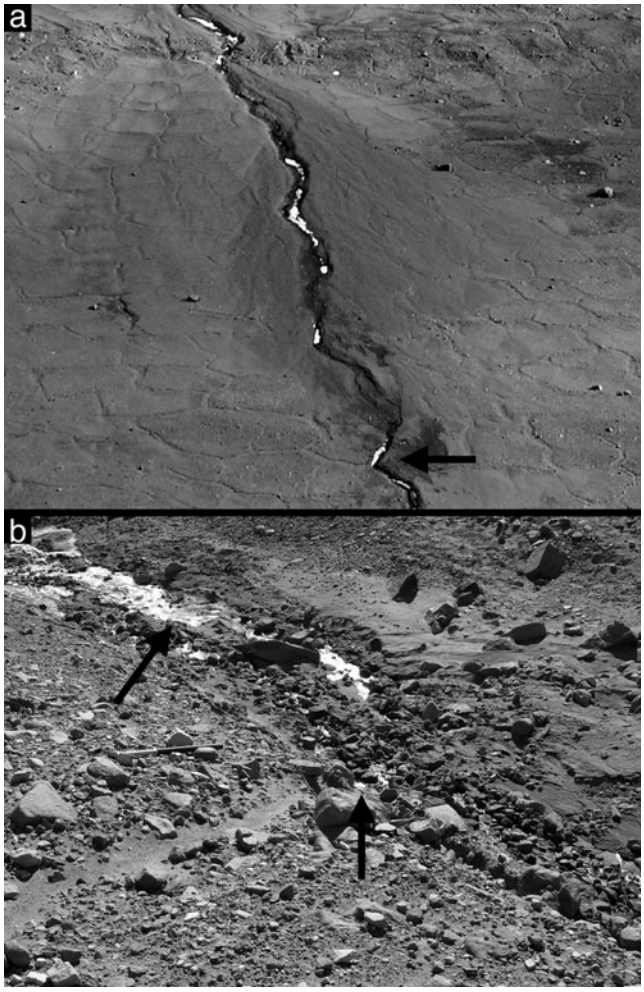

Fig. 14. a. Aerial view of a section of gully 1 showing a section of channel kinked at close to 120° (indicated by arrow). This type of channel morphology is interpreted as an indication of annexation of a pre-existing polygon trough. **b.** Surface view of an annexed polygon trough. A rocky-top polygon trough enters the frame from the lower left, bends to near-vertical at a hexagonal intersection near image centre, and bends towards the left (down-slope), exiting the frame at the upper left. A gully channel, containing surface flow, enters the frame from the lower right, encounters the polygon trough at image centre, and annexes the trough. Flowing liquid water is present in the polygon trough at the upper left (arrow), indicated by surface glare between small snow patches.

https://doi.org/10.1017/S0954102008001375 Published online by Cambridge University Press

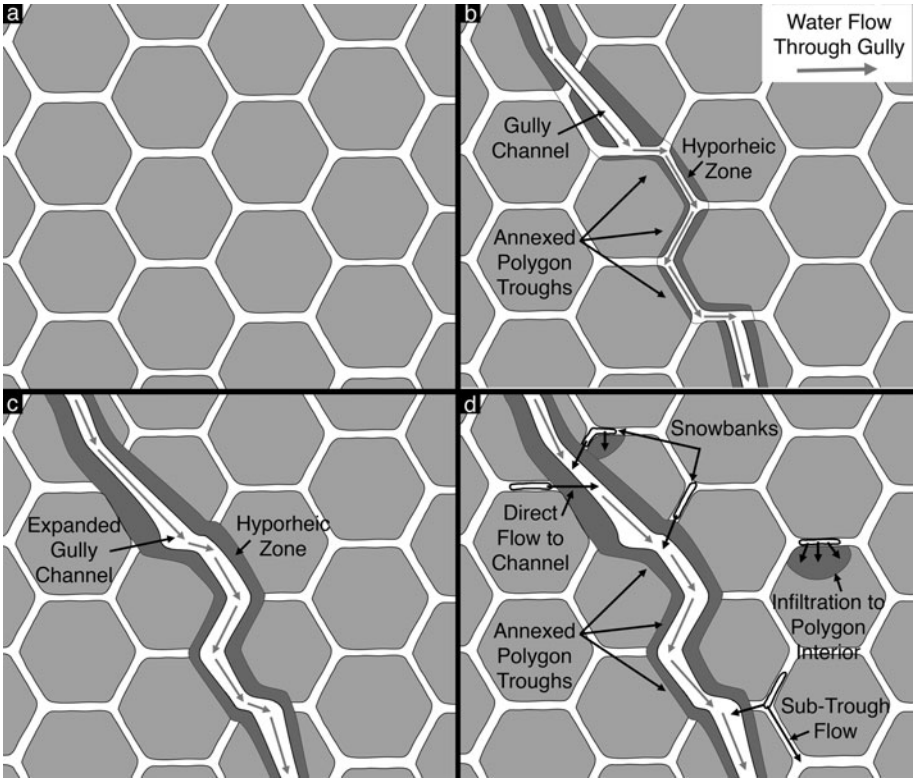

Fig. 15. Schematic diagram of polygon trough annexation and water movement in gully-polygon systems. **a.** The initial surface covered in thermal contraction crack polygons. **b.** An eroding gully channel encounters a polygon trough. Gully channel flow debouches into the trough and flows through the polygon trough network. We term this process polygon trough annexation. **c.** The annexed polygon troughs widen, deepen, and become more sinuous than neighbouring polygon troughs as the gully channel erodes the annexed troughs. **d.** Polygon troughs accumulate windblown snowbanks. Melting of snowbanks immediately adjacent to the gully channel provides a direct source of water to the gully channel. Some snowbank meltwater infiltrates polygon interiors; some snowbank meltwater flows along the ice-cement table beneath polygon troughs until it infiltrates a polygon interior, refreezes as part of a composite wedge, or contributes to gully channel flow.

polygon troughs, or through lateral hyporheic zones, water can be delivered to gully systems. Where water collects in troughs that are oriented perpendicular to the down-slope direction, water may pool, saturating the active layer, and promoting local solifluction.

Additionally, in locations where water sources are great enough to produce overland, or integrated overland/active-layer flow (Dickson *et al.* 2007, Head *et al.* 2007b, Levy *et al.* 2007a, Morgan *et al.* 2007), polygons may become directly incorporated into evolving gullies. Where a gully channel intersects a down-slope oriented polygon trough, meltwater flow can be transferred into the polygon trough (Figs 14 & 15). Evidence of this "annexation" of polygon troughs is based on direct observation of surface flow travelling from gully channels into appropriately oriented polygon troughs (Fig. 14). Supporting evidence for this annexation also comes from the observation of stratified, waterlain sediment in gully-channel polygon troughs. Where gully channels annex polygon troughs, overland, channelized flow is observed for tens of metres, until the polygon trough ceases to be oriented down-slope (commonly as a result of an orthogonal intersection with a trough oriented along strike). The surface flow either infiltrates into the polygon interior material, or a gully channel re-emerges, incising the polygon interior. Annexed portions of polygon troughs are generally widened and are commonly sinuous on $\sim$1 m wavelengths. Intersections between annexed troughs and adjoining polygon troughs are commonly rounded or bent, rather than sharp. In this manner, polygonally patterned ground directly affects the evolution of gullies in the South Fork study area. Reciprocally, polygon trough annexation is also an example of gully evolution modifying polygon morphology (Fig. 15).

Water storage

Water flowing through mapped gullies accumulates in distal and marginal hyporheic zones (Dickson *et al.* 2007, Head *et al.* 2007b, Levy *et al.* 2007a, Morgan *et al.* 2007), where it can affect local scale geomorphology. Both marginal and distal hyporheic zones are commonly surfaced with polygons: wet-top polygons, distally (i.e. in the down-slope direction), and rocky-top polygons, marginally.

Spatial partitioning of water in wet-top polygons is evidenced by the correlation of grain size and soil water content. In wet-top polygons, water is stored preferentially in polygon interiors, and is depleted in polygon wedges. This partitioning is interpreted to be a result of the higher specific retention of wet-top polygon interior material (on account of an unusually high fine fraction) as compared to wet-top polygon wedge material (which has a very high pebble fraction). The presence of a fine fraction in wet-top polygon interiors, and the resulting increase in specific retention, makes wet-top polygon interior material

https://doi.org/10.1017/S0954102008001375 Published online by Cambridge University Press

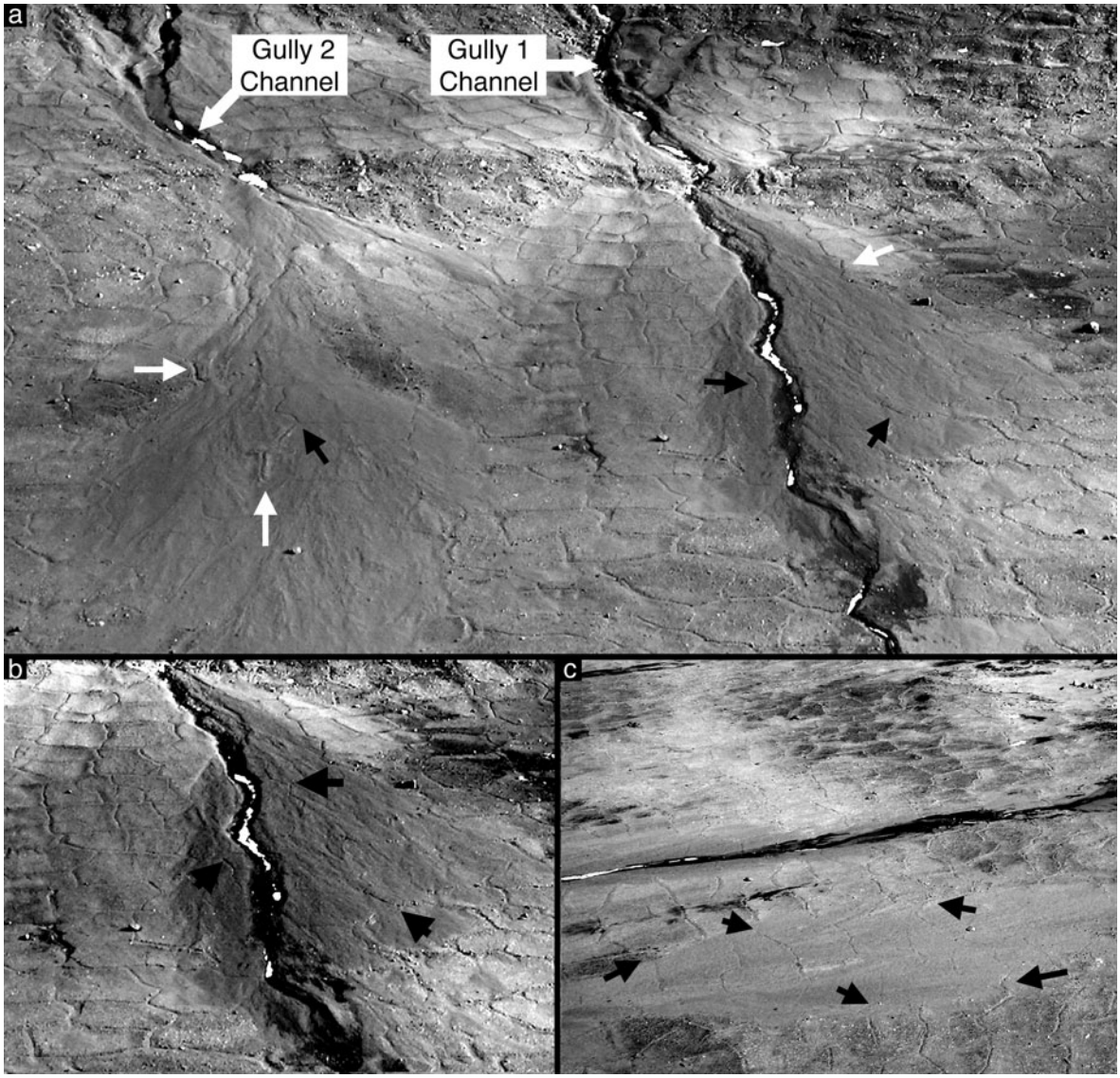

Fig. 16. a. Aerial view of gully 1 (right) and gully 2 (left) fans. White arrows indicate embayment (covering and surrounding) relationships of fan material over rocky-top polygon surfaces, usually associated with fan material being dammed by, or surrounding, locally-elevated rocky-top polygons. Black arrows point to surface fissures in the fan surface indicative of dissection of the fan by expanding thermal contraction cracks. Fine fissure networks can be traced to the surrounding rocky-top polygon network. **b.** Close-up, contrast-enhanced view of the gully 1 fan surface. Arrows indicate fissures in the fan surface associated with dissection of the fan by underlying, expanding polygon cracks. **c.** Close-up view of a down-slope portion of the gully 2 fan. Arrows indicate fissures in the fan surface which can be traced to fan-adjacent, non-overprinted rocky-top polygon troughs.

an efficient storage medium for distal hyporheic zone water. Exceptionally coarse wedge material (with Md50 approaching -1.6 ϕ) suggests that the wedges may be particularly well drained, or that enhanced communication with the atmosphere speeds the diffusion and evaporation of water present in the wedge. In addition, enhanced water retention in polygon centres may help localize and facilitate freeze-thaw processes. The latter is corroborated by the observation of frost-heaved cobbles and small boulders in the distal hyporheic zone and within the gully channels during an abrupt cooling event after gully channel flow had ceased for the season.

Polygon-gully stratigraphic relationships

Did the gullies form over continuous permafrost, indicative of climate conditions similar to present conditions, or did they form during a warmer, and wetter set of microclimate conditions? On the basis of the stratigraphic relationships among gullies and polygons, we show that patterned

https://doi.org/10.1017/S0954102008001375 Published online by Cambridge University Press

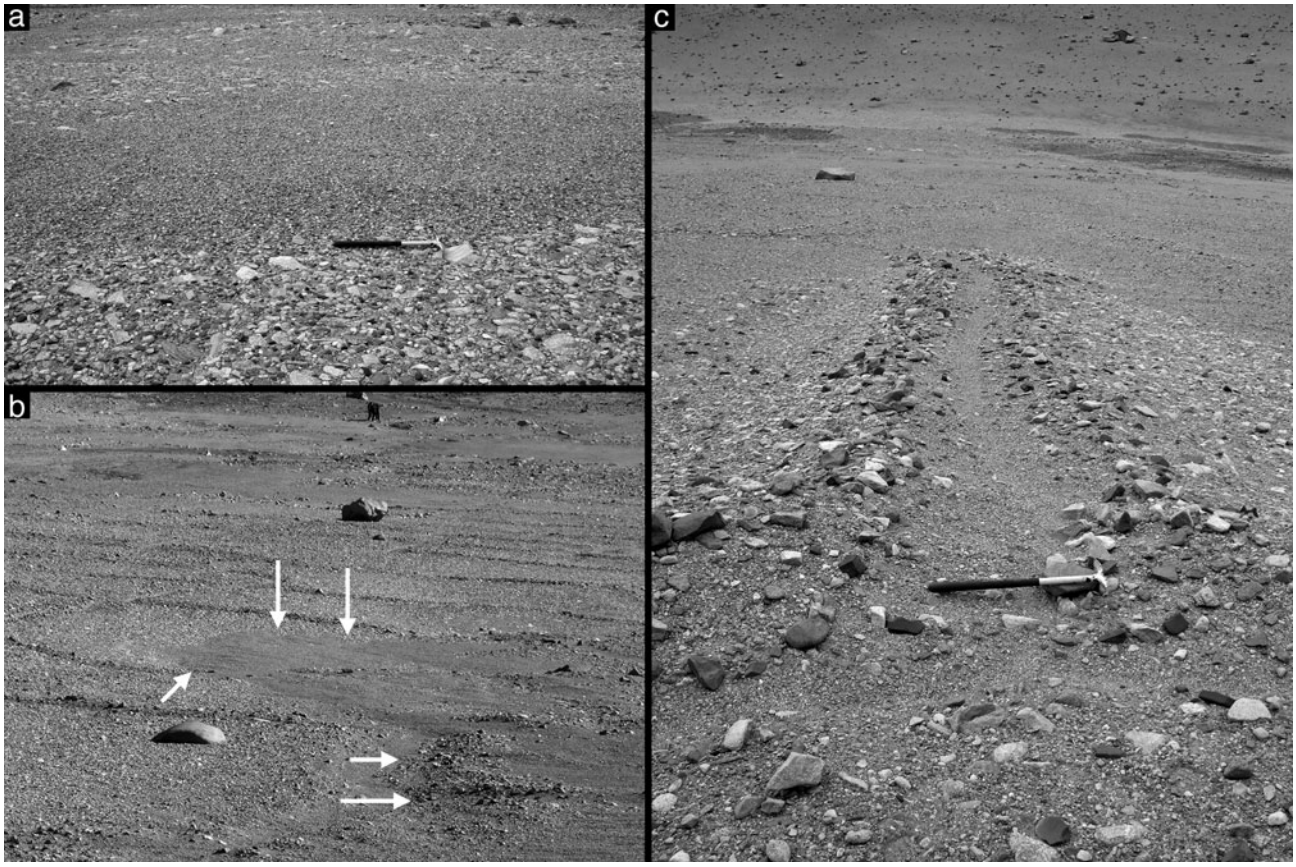

Fig. 17. a. Surface view of the contact between fan material (finer-grained, midground) and rocky-top polygon desert pavement (cobble-sized grains, foreground and background). A pick, 60 cm long, marks the proximal contact. **b.** Embaying relationships between fan material and rocky-top polygons in the gully 2 fan. White arrows indicate topographic obstacles which served as an impediment to fan expansion. **c.** Outcrop of a well-formed rocky-top polygon trough (image centre, marked by pick) and shoulders (surfaced by cobble-size desert pavement), surrounded by finer-grained fan material.

ground pre-dates, evolved concurrently with, and post-dates gully features in the South Fork study area, strongly suggesting the continued presence of an impermeable, ice-cemented layer beneath the gully channels and fans during the course of their formation and evolution.

Gully-channel/polygon relationships

As illustrated above, polygon troughs commonly intersect gully channels in the South Fork study area (Figs 11 & 12). Determining whether the channels cross-cut the troughs, or whether the polygon fractures formed after channel emplacement is essential to determine relative ages. In many locations, polygon troughs terminate in near-orthogonal intersections with gully channels. Wedge cross-sections are commonly exposed in the banks at such locations, but are degraded by wasting of the gully banks. Polygon fractures commonly initiate orthogonally to fluvial/lacustrine systems on account of the moderation of thermal conditions produced by liquid water (Lachenbruch 1962). However, the observation of well formed polygon wedges exposed at these orthogonal intersections with gully channels suggests erosion of pre-existing wedges at the channel banks, rather than pinching out of post-gully contraction cracks. Further, in many locations, well formed polygon troughs intersect the gully channel at non-orthogonal intersection angles. Oblique intersections are not expected if fractures formed subsequent to channel incision. Obliquely intersecting polygon troughs commonly occur in areas with limited marginal hyporheic zones, suggesting that stresses associated with polygon formation were little affected by the presence of proximate hyporheic moisture. Further, in locations with little bank erosion, polygon troughs intersecting gully channels occur with matching troughs present on the opposite bank of the gully channel. There is no *a priori* reason to expect polygon troughs forming subsequent to gully channel incision to commonly intersect the gully at the same location. Lastly, in some locations, the gully channels are angular and follow polygon spacing (Fig. 14), suggesting that present gully channels are, in locations, annexing former polygon troughs (see previous section). Taken together, these

https://doi.org/10.1017/S0954102008001375 Published online by Cambridge University Press

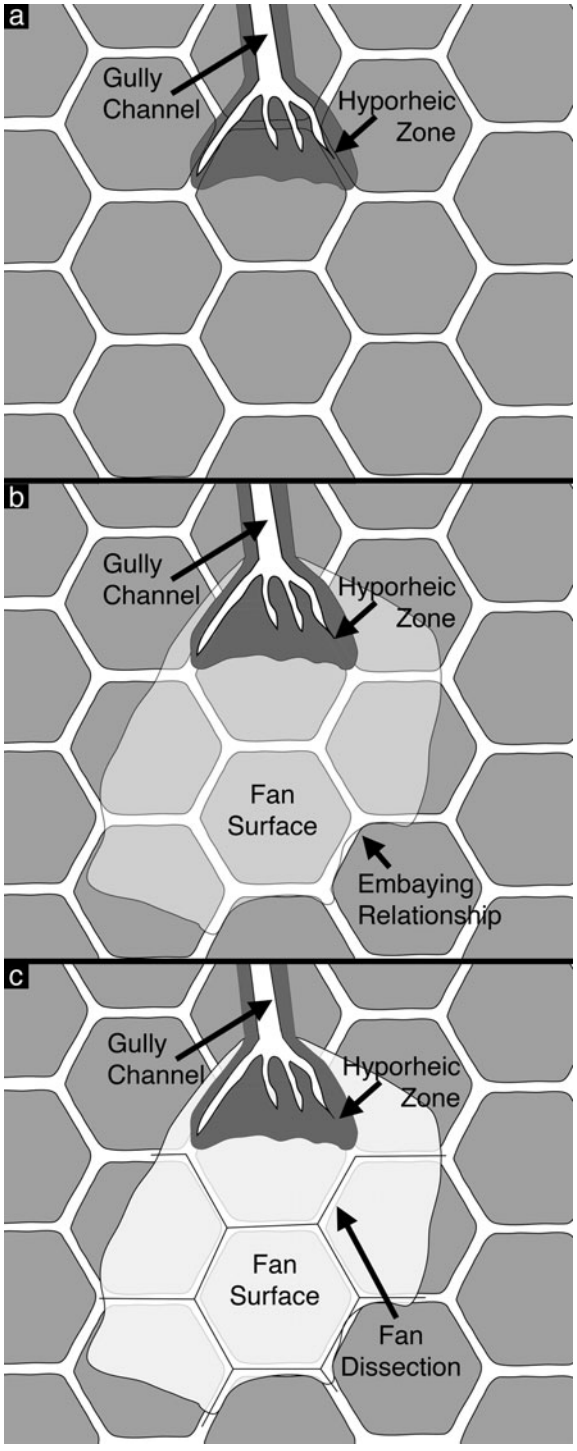

Fig. 18. Schematic diagram illustrating relationships between gully fans and polygons. **a.** The distal end of the gully extends into previously extant thermal contraction crack polygons. **b.** Gully-transported materials are deposited in a fan structure over the polygons. The fan embays high polygon topography and is in places arrested by the presence of polygon troughs. **c.** As the fan surface aggrades and thickens, thermal contraction keeps pace with fan growth, resulting in the formation of a network of fine cracks in the fan surface that are contiguous with the surrounding polygon network.

observations suggest that gully channel incision occurred in the presence of thermal contraction crack polygons and that suitably oriented polygon troughs have been annexed by evolving gully channels.

Gully-fan/polygon relationships

Contacts between gully fan surfaces and inter-gully surfaces can be used to trace the stratigraphic relationships between gully fans and polygons in the South Fork study area (Figs 16 & 17). Mapped spatial contacts between gully fan deposits and inter-gully surfaces are marked by an abrupt transition between cobble-armoured pavements (typical of inter-fan rocky-top polygons) and pebble-armoured fan surfaces (Figs 16 & 17). Aerial identification of the fan/inter-gully contact is marked by an increase in topography on the fan surface, and an apparent smoothing of rocky-top polygon textures (Fig. 16).

Stratigraphic relationships between the fans at the base of gullies 1 and 2, and the surrounding polygons suggest 1) that the fans were emplaced on top of pre-existing polygons, and 2) that polygon growth continued unabated during fan aggradation. First, rocky-top polygons are directly overlain by well-sorted fan material (Figs 16 & 17). At some contacts between the fan surfaces and the inter-gully surface, fan material onlaps the raised shoulders of rocky-top polygons, suggesting that the raised rocky-top polygon shoulder acted as a barrier to fan deposition (Figs 16 & 17). At other contacts between the fan surfaces and the inter-gully surface, fan material enters into rocky-top polygon troughs, suggesting that the trough depression acted as a topographic barrier to fan expansion. Lastly, within the gully 2 fan surface itself, isolated patches of pristine, cobble-paved, rocky-top polygons are present on local topographic highs within the fan surface, surrounded on all sides by fan material.

Additionally, the fans show a network of < 3 cm wide surface cracks, of comparable diameter, spacing, and patterning to rocky-top polygons in the adjacent inter-fan surface (Fig. 16). This suggests that the fine cracks are a direct extension of the underlying polygon network. Although subdued, the underlying rocky-top polygon network can be traced clearly across the entire width of the gully 2 fan (Fig. 16), suggesting that thermal contraction cracks extend upward into fan material. Fractures "kept pace" with the aggradation of fan materials, a phenomenon similar to that observed in Murton & Bateman (2007). Gully fan deposition and evolution on a polygonally patterned surface is illustrated schematically in Fig. 18.

Conclusions and implications

Thermal contraction crack polygons in the South Fork of Wright Valley were analysed as a component of a

https://doi.org/10.1017/S0954102008001375 Published online by Cambridge University Press

near-surface hydrological system in which gullies form under cold-desert conditions. Composite-wedge polygon morphological variations were found to form a sequence of fluvial modification from largely unmodified composite-wedge polygons (dolerite tongue polygons, some rocky-top polygons) to polygons which could only form as part of a gully system (gully channel and wet-top polygons). Polygonally patterned ground in the South Fork study area was found to play a significant role in the accumulation, transport, and storage of gully meltwater. The presence of a continually frozen and impermeable ice-cement layer was confirmed, suggesting that most water present in the South Fork region active layer is derived from summertime melting of accumulated snow. Modification of polygonally patterned ground surface morphology was observed, and is consistent with accumulation and flow of water along the depressed ice-cement table beneath polygon troughs. Gully-polygon stratigraphic relationships indicate that polygonal patterning preceded gully formation, and continued throughout gully evolution. This implies the enduring existence of climate conditions permitting the growth of composite-wedge polygons, and further implies the continuous presence of an impermeable ice-cemented substrate during the entire course of gully evolution.

This analysis suggests that polygon troughs represent an additional flow path for water in the McMurdo Dry Valleys hydrological systems, both as part of an extended hyporheic zone and as an intermediary between snowbanks and overland flow. This flow path extends the time and space during which weathering and distillation reactions can occur, contributing to solute load, isotopic fractionation, and the biological potential of near-surface waters (e.g. Gooseff *et al.* 2002, Harris *et al.* 2007).

Lastly, this analysis provides a framework for understanding the relationships between polygonally patterned ground observed on gullied slopes on Mars (e.g. Bridges & Lackner 2006, Levy *et al.* 2007b). If comparable stratigraphic relationships between Martian gully subsystems (alcoves, channels, and fans) and polygons can be documented, then the presence of a continuous, impermeable, ice-cemented, permafrost layer beneath the gullies can be inferred, strongly suggesting an atmospherically derived (niveal, frost deposition, etc.) source for Martian gully-carving fluids.

Acknowledgements

This work was made possible with support of JSL by the Rhode Island Space Grant Consortium, by NSF Grant ANT-0338291 to DRM and JWH, and NASA MFRP Grant NNX06AE32G to DRM and JWH. Thanks to James Dickson, Douglas Kowalewski, Gareth Morgan, David Shean, and Kate Swanger for field support. Thanks to two anonymous reviewers. Also, thanks to the helicopter pilots, technicians, and ground crew of PHI, Inc, as well as to the staff of Raytheon Polar Services Company, and the personnel of McMurdo Station.

References

Berg, T.E. & Black, R.F. 1966. Preliminary measurements of growth of non-sorted polygons, Victoria Land, Antarctic. *Antarctic Research Series*, **8**, 61–108.

Black, R.F. 1982. Patterned-ground studies in Victoria Land. *Antarctic Journal of the United States*, **17** (5), 53–54.

Bridges, N.T. & Lackner, C.N. 2006. Northern hemisphere Martian gullies and mantled terrain: implications for near-surface water migration in Mars' recent past. *Journal of Geophysical Research*, **111**, 10.1029/2006/JE002702.

Burt, D.M. & Knauth, L.P. 2007. Impacts, salts, and ice on Mars: how brine flow in young gullies and elsewhere could be related to impact cratering. *In 38th Lunar and Planetary Science Conference*, League City, TX. Abstract #2054, www.lpi.usra.edu/meetings/lpsc2007/pdf/2054.pdf

Dickson, J.L., Head, J.W., Marchant, D.R., Morgan, G.A. & Levy, J.S. 2007. Recent gully activity on Mars: Clues from late-stage water flow in gully systems and channels in the Antarctic Dry Valleys. *In 38th Lunar and Planetary Science Conference*, League City, TX. Abstract #1678, www.lpi.usra.edu/meetings/lpsc2007/pdf/1678.pdf.

Fortier, D., Allard, M. & Shur, Y. 2007. Observation of rapid drainage system development by thermal erosion of ice wedges on Byot Island, Canadian Arctic Archipelago. *Permafrost and Periglacial Processes*, **18**, 229–243.

Gooseff, M.N., McKnight, D.M., Lyons, W.B. & Blum, A.E. 2002. Weathering reactions and hyporheic exchange controls on stream water chemistry in a glacial meltwater stream in the McMurdo Dry Valleys. *Water Resources Research*, **38**, 10.1029/2001WR000834.

Harris, K.J., Carey, A.E., Lyons, W.B., Welch, K.A. & Fountain, A.G. 2007. Solute and isotope geochemistry of subsurface ice melt seeps in Taylor Valley, Antarctica. *Geological Society of America Bulletin*, **119**, 548–555.

Head, J.W., Marchant, D.R., Dickson, J.L., Levy, J.S. & Morgan, G.A. 2007a. Mars Gully analogs in the Antarctic Dry Valleys: geological setting and processes. *In 38th Lunar and Planetary Science Conference*, League City, TX. Abstract #1617, www.lpi.usra.edu/meetings/lpsc2007/pdf/1617.pdf.

Head, J.W., Marchant, D.R., Dickson, J.L., Levy, J.S. & Morgan, G.A. 2007b. Slope streaks in the Antarctic Dry Valleys: characteristics, candidate formation mechanism, and implications for slope streak formation in the Martian environment. *In 38th Lunar and Planetary Science Conference*, League City, TX. Abstract #1935, www.lpi.usra.edu/meetings/lpsc2007/pdf/1935.pdf.

Isaac, M.J., Chinn, T.J., Edbrook, S. & Forsyth, J. 1996. *Geology of the Olympus Range area, southern Victoria Land, Antarctica*. Wellington: Institute of Geological and Nuclear Sciences, 60 pp.

Kowalewski, D.E., Marchant, D.R., Head, J.W. & Levy, J.S. 2007. Modeling vapour diffusion in sublimation tills of the Antarctic Dry Valleys: implications for the preservation of near-surface ice on Mars. *In 38th Lunar and Planetary Science Conference*, League City, TX. Abstract #2143, www.lpi.usra.edu/meetings/lpsc2007/pdf/2143.pdf.

Kowalewski, D.E., Marchant, D.R., Levy, J.S. & Head, J.W. 2006. Quantifying low rates of summertime sublimation for buried glacier ice in Beacon Valley, Antarctica. *Antarctic Science*, **18**, 421–428.

Lachenbruch, A.H. 1962. Mechanics of thermal contraction cracks and ice-wedge polygons in permafrost. *Geological Society of America Special Papers*, **70**, 1–69.

Lachenbruch, A.H. 1963. Contraction theory of ice-wedge polygons: a qualitative discussion. *In International Permafrost Conference, Proceedings*, Lafayette, Indiana. Washington, DC: National Academy of Sciences, National Research Council Publication, 1287, 63–71.

Leffingwell, E. de K. 1915. Ground-ice wedges: the dominant form of ground-ice on the north coast of Alaska. *Journal of Geology*, **23**, 635–654.

Levy, J.S., Head, J.W. & Marchant, D.R. 2005. The origin and evolution of oriented-network polygonally patterned ground: the Antarctic Dry Valleys as Mars Analogue. *In 36th Lunar and Planetary Science Conference*, League City, TX. Abstract #1334, www.lpi.usra.edu/meetings/lpsc2005/pdf/1334.pdf.

Levy, J.S., Head, J.W., Marchant, D.R., Morgan, G.A. & Dickson, J.L. 2007a. Gully surface and shallow subsurface structure in the south fork of Wright Valley, Antarctic Dry Valleys: implications for gully activity on Mars. *In 38th Lunar and Planetary Science Conference*, League City, TX. Abstract #1728, www.lpi.usra.edu/meetings/lpsc2007/pdf/1728.pdf.

Levy, J.S., Head, J.W., Marchant, D.R., Morgan, G.A. & Dickson, J.L. 2007b. Gully-polygon interactions and stratigraphy on Earth and Mars: sand-wedge polygons as part of cold-desert, near-surface fluvial systems. *In Seventh International Conference on Mars*, Pasadena, CA, www.lpi.usra.edu/meetings/7thmars2007/pdf/3059.pdf.

Lyons, W.B., Welch, K.A., Carey, A.E., Wall, D.H., Virginia, R.A., Fountain, A.G., Doran, P.T., Csatho, B.M. & Tremper, C.M. 2005. Groundwater seeps in Taylor Valley, Antarctica: an example of a subsurface melt event. *Annals of Glaciology*, **40**, 200–207.

Malin, M.C. & Edgett, K.S. 2001. Mars Global surveyor Mars Orbiter camera: interplanetary cruise through primary mission. *Journal of Geophysical Research*, **106**, 23 429–23 540.

Marchant, D.R. & Head, J.W. 2007. Antarctic Dry Valleys: microclimate zonation, variable geomorphic processes, and implications for assessing climate change on Mars. *Icarus*, **192**, 187–222.

Marchant, D.R., Lewis, A.R., Phillips, W.M., Moore, E.J., Souchez, R.A., Denton, G.H., Sugden, D.E., Potter, N.J. & Landis, G.P. 2002. Formation of patterned ground and sublimation till over Miocene glacier ice in Beacon Valley, southern Victoria Land, Antarctica. *Geological Society of America Bulletin*, **114**, 718–730.

Masch, F.D. & Denny, K.J. 1966. Grain size distribution and its effect on the permeability of unconsolidated sands. *Water Resources Research*, **2**, 665–677.

McGinnis, L.D. & Jensen, T.E. 1971. Permafrost-hydrogeologic regimen in two ice-free valleys, Antarctica, from electrical depth sounding. *Quaternary Research*, **1**, 31–38.

McKay, C.P., Mellon, M.T. & Friedman, E.I. 1998. Soil temperatures and stability of ice-cemented ground in the McMurdo Dry Valleys, Antarctica. *Antarctic Science*, **10**, 31–38.

McKnight, D.M., Niyogi, D.K., Alger, A.S., Bomblies, A., Conovitz, P.A. & Tate, C.M. 1999. Dry valley streams in Antarctica: ecosystems waiting for water. *BioScience*, **49**, 985–995.

Mellon, M.T. 1997. Small-scale polygonal features on Mars: seasonal thermal contraction cracks in permafrost. *Journal of Geophysical Research*, **102**, 25 617–25 628.

Morgan, G.A., Head, J.W., Marchant, D.R., Dickson, J.L. & Levy, J.S. 2007. Gully formation on Mars: testing the snowpack hypothesis from analysis of analogs in the Antarctic Dry Valleys. *In 38th Lunar and Planetary Science Conference*, League City, TX. Abstract #1656, www.lpi.usra.edu/meetings/lpsc2007/pdf/1656.pdf.

Murton, J.B. & Bateman, M.D. 2007. Syngenetic sand veins and anti-syngenetic sand wedges, Tuktoyaktuk coastlands, Western Arctic Canada. *Permafrost and Periglacial Processes*, **18**, 33–47.

Péwé, T.L. 1959. Sand-wedge polygons (tessellations) in the McMurdo Sound region, Antarctica - a progress report. *American Journal of Science*, **257**, 545–552.

Péwé, T.L. 1974. Geomorphic processes in polar deserts. *In* Smiley, T.L. & Zumberge, J.H. *eds*. *Polar deserts and modern man*. Tucson, AZ: University of Arizona Press, 35–52.

Ragotzkie, R.A. & Likens, G.E. 1964. The heat balance of two Antarctic lakes. *Limnology and Oceanography*, **9**, 412–425.

Riordan, A.J. 1973. The climate of Vanda Station, Antarctica. *In* Raasch, G.O., *ed*. *Geology of the Arctic*. Toronto: University of Toronto Press, 268–275.

Sheldrick, B.H. & Wang, C. 1993. Particle size distribution. *In* Carter, M.R., *ed*. *Soil sampling and methods of analysis*. Boca Raton, FL: Lewis Publishers, 499–511.

Summers, W.K. & Weber, P.A. 1984. The relationship of grain-size distribution and hydraulic conductivity - an alternate approach. *Ground Water*, **22**, 474–475.

Thompson, D.C. 1973. Climate of the Dry Valleys area of southern Victoria Land. *New Zealand Geographical Society Conference Series*, **4**, 259–265.

Topp, G.C. 1993. Soil water content. *In* Carter, M.R., *ed*. *Soil sampling and methods of analysis*. Boca Raton, FL: Lewis Publishers, 541–557.

Wentworth, S.J., Gibson Jr, E.K. & McKay, D.S. 2003. Low-temperature, aqueous alteration of soil in Wright Valley, Antarctica, compared with aqueous alteration on Mars. *In Third Mars Polar Science Conference*, Alberta, Canada. Abstract #8128, www.lpi.usra.edu/meetings/polar2003/pdf/8128.pdf.